

注水誘発地震の統計的な特徴

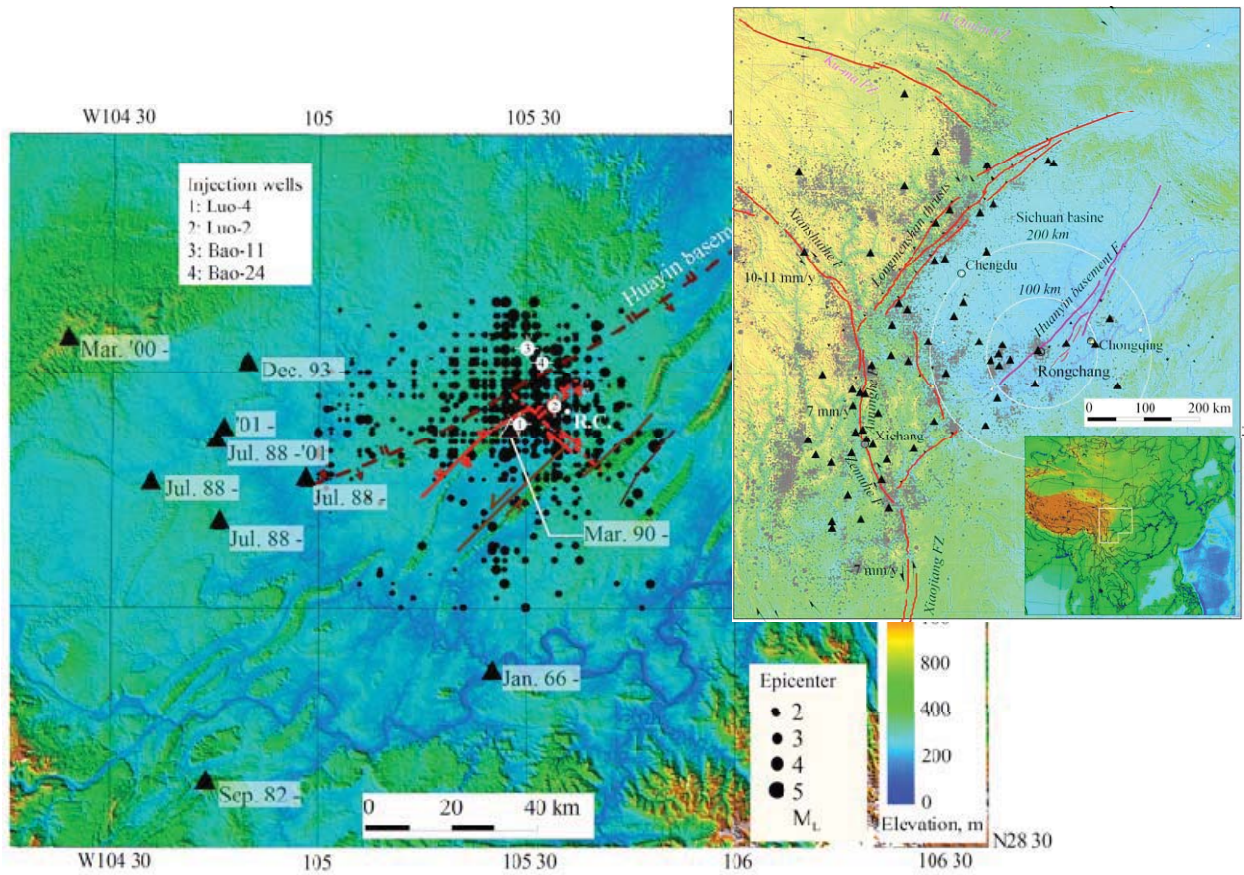


図2 荣昌天然ガス田排水圧入井の位置、断層、地震観測点および地震の分配を示す。

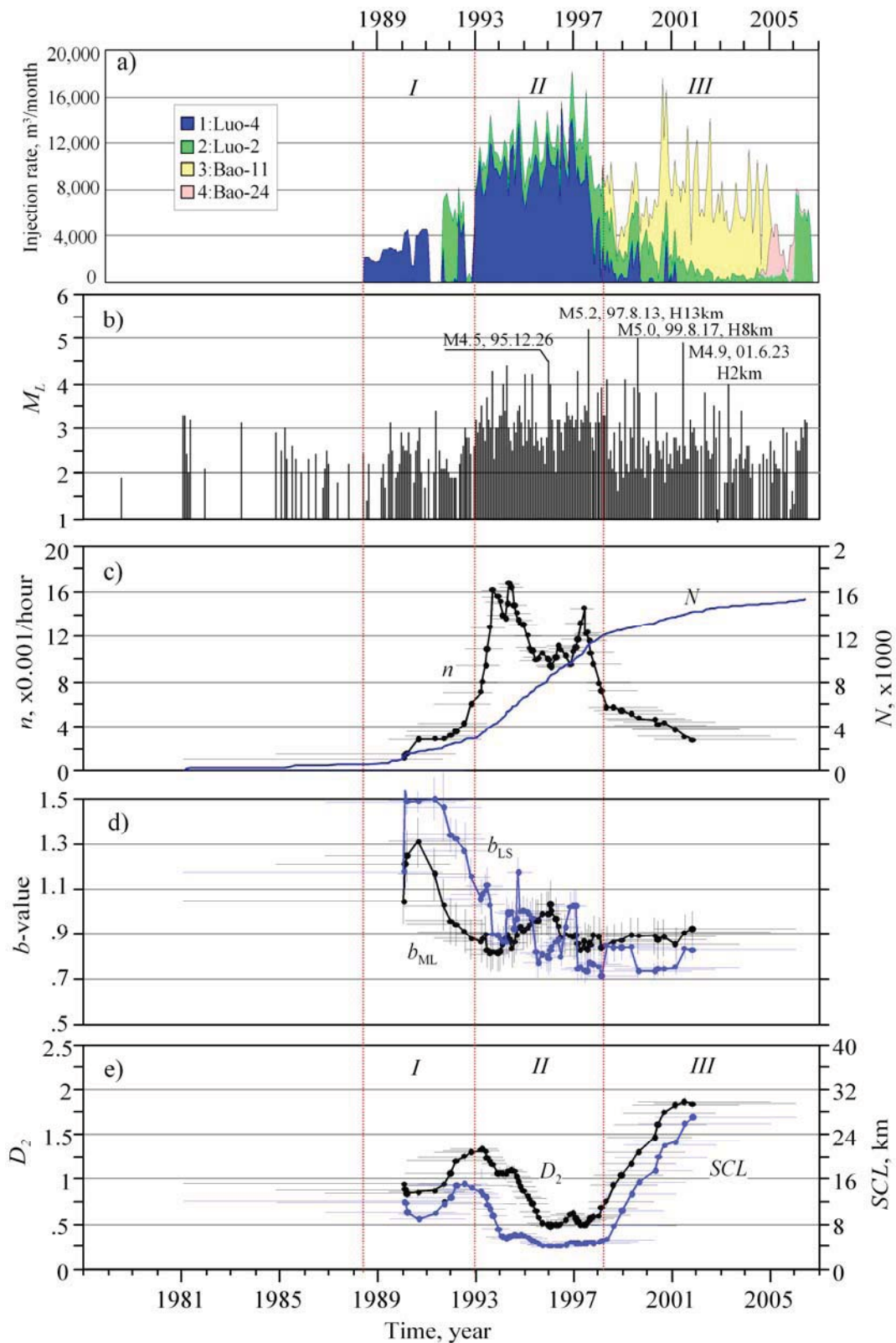


図3 注水履歴、地震時系列及び主な統計パラメータの時間変化を示す。(a)月間注水量。(b)地震マグニチュード。(c)地震発生頻度と積算値。(d)地震頻度-規模分布における b 値。(e)震源分布の空間相関距離(SCL)とフラクタル次元(D_2)。

Fig.3 Temporal trends in the injection rate and the magnitude and major statistics of earthquakes within the SEA (Sichuan Earthquake Administration) catalog. (a) Monthly volume of injected water. (b) Magnitude of earthquakes. (c) Event rate (n) and cumulative event number (N). (d) The b value in the frequency-magnitude distribution estimated using the least squares method and the maximum likelihood method. (e) Spatial correlation length (SCL) derived from single-link cluster analysis and the fractal dimension (D_2) of the hypocenter distribution. Values in (c)–(e) were

calculated sequentially for consecutive groups of 200 events with a running step of 20 events.

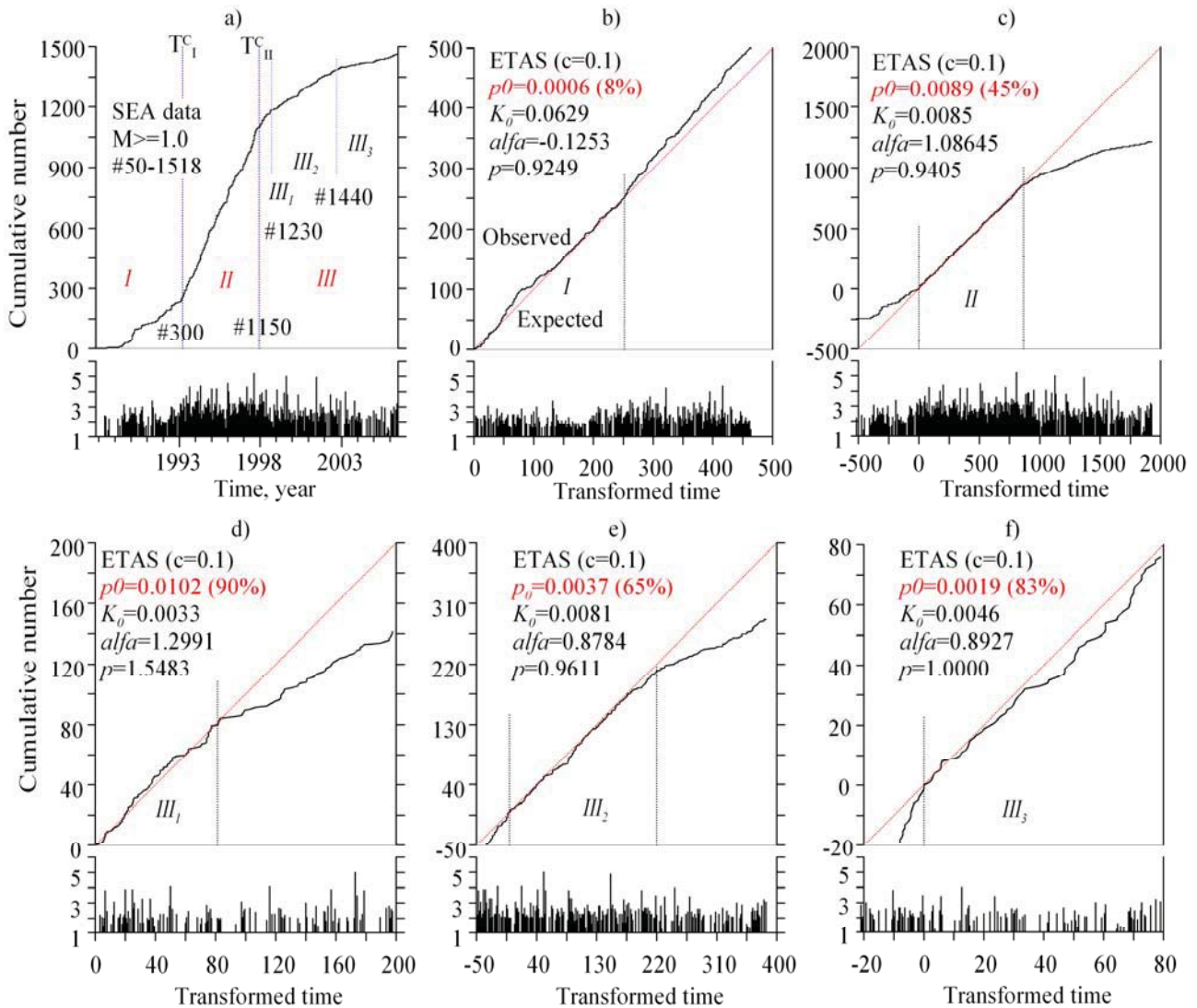


図 5 ETAS モデリング結果。図 3 に示している特徴的なフェーズと良く一致する地震活動の変化点が抽出され、それぞれのフェーズでの地震活動が異なる特徴が示される。フェーズ I では 8%の地震が外部的に（つまり注水）引き起こされ、残りは大森-タイプの自己誘発活動である。p0 はランダム成分で、p0 が高いほど外部的トリガーの役割対大森-タイプの自己誘発の役割が大きい。

Fig.5 Summary of the results of epidemic-type aftershock sequence (ETAS) modeling. (a) Two major change points in earthquake activity (TcI and TcII) and three major phases of activity defined by the change points (I, II, and III) are identified. Two change subpoints are identified in phase III; hence, phase III contains three subphases (III1, III2, and III3). (b-d) Estimated ETAS parameters for each phase and subphase. The cumulative number of earthquakes as a function of time or transformed time (events) is compared with that predicted by the ETAS model..